HHS Public Access

Author manuscript

Nature. Author manuscript; available in PMC 2019 August 12.

Published in final edited form as:

Nature. 2013 April 11; 496(7444): 219–223. doi:10.1038/nature12018.

Diverging neural pathways assemble a behavioural state from separable features in anxiety

Sung-Yon Kim[1,2,*], **Avishek Adhikari**[1,*], **Soo Yeun Lee**[1,3], **James H. Marshel**[1], **Christina K. Kim**[1,2], **Caitlin S. Mallory**[1,2], **Maisie Lo**[1], **Sally Pak**[1], **Joanna Mattis**[1,2], **Byung Kook Lim**[4], **Robert C. Malenka**[4], **Melissa R. Warden**[1], **Rachael Neve**[5], **Kay M. Tye**[1,5], **Karl Deisseroth**[1,2,3,4,6]

[1]Department of Bioengineering, Stanford University, Stanford, California 94305, USA.

[2]Neurosciences Program, Stanford University, Stanford, California 94305, USA.

[3]CNC Program, Stanford University,Stanford, California 94305, USA.

[4]Department of Psychiatry and Behavioral Sciences, Stanford University, Stanford, California 94305, USA.

[5]Department of Brain and Cognitive Sciences, Massachusetts Institute of Technology, Cambridge, Massachusetts 02139, USA.

[6]Howard Hughes Medical Institute, Stanford University, Stanford, California 94305, USA.

Abstract

Behavioural states in mammals, such as the anxious state, are characterized by several features that are coordinately regulated by diverse nervous system outputs, ranging from behavioural choice patterns to changes in physiology (in anxiety, exemplified respectively by risk-avoidance and respiratory rate alterations)[1,2]. Here we investigate if and how defined neural projections arising from a single coordinating brain region in mice could mediate diverse features of anxiety. Integrating behavioural assays, *in vivo* and *in vitro* electrophysiology, respiratory physiology and optogenetics, we identify a surprising new role for the bed nucleus of the stria terminalis (BNST) in the coordinated modulation of diverse anxiety features. First, two BNST subregions were unexpectedly found to exert opposite effects on the anxious state: oval BNST activity promoted several independent anxious state features, whereas anterodorsal BNST-associated activity exerted anxiolytic influence for the same features. Notably, we found that three distinct anterodorsal BNST efferent projections—to the lateral hypothalamus, parabrachial nucleus and ventral tegmental area—each implemented an independent feature of anxiolysis: reduced risk-avoidance,

Correspondence and requests for materials should be addressed to K.D. (deissero@stanford.edu).

*These authors contributed equally to this work.

Author Contributions S.-Y.K., A.A. and K.D. designed the study, interpreted results and wrote the paper. S.-Y.K. coordinated the experiments. S.-Y.K, A.A., S.Y.L., C.S.M., M.R.W. and K.M.T. performed optogenetic behavior and electrophysiology experiments. S.-Y.K., M.L., S.P. and J.M. performed immunohistochemistry. J.H.M. and C.K.K. performed calcium imaging. B.K.L., R.C.M. and R.N. provided viruses. All authors contributed to editing. K.D. supervised all aspects of the project.

The authors declare competing financial interests: details accompany the full-text HTML version of the paper at www.nature.com/nature. Readers are welcome to comment on the online version of the paper.

Supplementary Information is available in the online version of the paper.

reduced respiratory rate, and increased positive valence, respectively. Furthermore, selective inhibition of corresponding circuit elements in freely moving mice showed opposing behavioural effects compared with excitation, and *in vivo* recordings during free behaviour showed native spiking patterns in anterodorsal BNST neurons that differentiated safe and anxiogenic environments. These results demonstrate that distinct BNST subregions exert opposite effects in modulating anxiety, establish separable anxiolytic roles for different anterodorsal BNST projections, and illustrate circuit mechanisms underlying selection of features for the assembly of the anxious state.

Animals encounter environmental conditions that require rapid switching among different behavioural states to increase the likelihood of survival and reproduction. Such states consist of a constellation of changes coordinated by distinct modalities of nervous system output[1,2], and understanding this behavioural-state assembly from diverse features is of fundamental interest. A well-studied example is fear, in which the amygdala is thought to modulate various aspects of fear expression by multiple downstream targets[1–4]. Here we tested whether specific diverging projections causally recruit separable features to coordinate a behavioural state, focusing on anxiety as a state not only important in normal and pathological behaviour[5], but also exhibiting many disparate features that are quantifiable in mice.

Evidence from anatomical[6–8], behavioural[9,10] and neuroimaging studies[11,12] has implicated the BNST in pathological and adaptive anxiety; for example, lesions of the dorsal BNST, henceforth referred to as BNST, have been reported to decrease anxiety-like behaviour[9,10]. To test this finding further, we infused glutamate receptor antagonists into the BNST before the elevated-plus maze (EPM)[10] test in mice (Fig. 1a; histology in Supplementary Figs 1–3). This intervention increased open-arm exploration ($P < 0.01$, see Supplementary Information for statistical analysis; Fig. 1a) without altering locomotion (Supplementary Fig. 4; such increased exploration of open spaces, to which mice exhibit innate aversion, is thought to represent reduced anxiety-like behaviour[13]). We next optogenetically inhibited the BNST using an enhanced form of the inhibitory *Natronomonas pharaonis* halorhodopsin (eNpHR3.0)[14] and delivery of yellow light to the BNST (eNpHR3.0:BNST somata; Fig. 1b); increased exploration of open spaces in the EPM test and open field test (OFT) was observed (Fig. 1b and Supplementary Fig. 5a, b), indicating anxiolysis. Conversely, stimulation of BNST somata with the excitatory channelrhodopsin-2 (ChR2) increased behavioural measures of anxiety in both assays (ChR2:BNST somata; Supplementary Fig. 6). To test whether this manipulation modulated physiological manifestations of anxiety, we stimulated BNST somata while monitoring respiratory rate; hyperventilation is linked to increased anxiety in humans[15,16] and rodents (Supplementary Fig. 7), and the BNST is known to project to respiratory centres[17,18]. Indeed, increased respiratory rate was observed (Supplementary Fig. 6d). Together these results suggest that activity in the BNST drives an anxiety-like state, consistent with most previous studies[9].

However, these results may not provide a complete picture of the BNST, which contains several subregions[7,19,20]. We next targeted the oval nucleus of the BNST (hereafter termed ovBNST), by introducing a Cre-dependent eNpHR3.0 virus into the BNST of dopamine

receptor 1a (Drd1a::Cre) mice that show restricted Cre expression in the ovBNST (eNpHR3.0:ovBNST; Fig. 1c). Yellow light delivery in eNpHR3.0:ovBNST mice decreased avoidance of EPM open arms ($P < 0.0001$; Fig. 1d) and the OFT centre ($P < 0.001$; Supplementary Fig. 5c). The same manipulation also decreased respiratory rate ($P < 0.05$; Fig. 1e). Conversely, stimulating the ovBNST with ChR2 increased both behavioural and physiological measures of anxiety (ChR2:ovBNST; Supplementary Fig. 8). These results suggested an anxiogenic role for the ovBNST, and were consistent with the results obtained by modulating the entire BNST (Fig. 1a, b).

We next investigated the function of basolateral amygdala (BLA) inputs to the BNST, as the BLA is a region implicated in anxiety[2,9] that projects to the BNST[7]. Mice expressing eNpHR3.0–eYFP in BLA pyramidal neurons displayed enhanced yellow fluorescent protein $(eYFP)^+$ fibres projecting to the region of the BNST surrounding the ovBNST, hereafter referred to as anterodorsal BNST, or adBNST[7] (eNpHR3.0: BLA-adBNST; Fig. 1f). Surprisingly, inhibiting the BLA-adBNST projection increased avoidance of EPM open arms ($P < 0.01$; Fig. 1g) and the OFT centre ($P < 0.01$; Supplementary Fig. 5e), and also increased respiratory rate ($P < 0.01$; Fig. 1h). Conversely, stimulating BLA inputs with ChR2 (ChR2:BLA-adBNST; Fig. 2a) decreased behavioural anxiety measures (Fig. 2b and Supplementary Figs 9a, b and 10) and respiratory rate ($P < 0.05$; Fig. 2c). Because the BLA projection is thought to be excitatory, as confirmed later, these data suggest that adBNST recruitment is anxiolytic, in contrast to the anxiogenic nature of ovBNST activity. Importantly, these effects were not attributable to excitation of BLA fibres in the anterior commissure (Supplementary Fig. 11). As an additional test, considering that a clinically relevant[21,22] feature of anxiolysis can be positive subjective valence, we asked whether stimulating BLA-adBNST projections could elicit positive conditioning valence (using the real-time place preference (RTPP) task; see Methods), but we did not observe elicited place preference (Fig. 2d).

Having found that driving adBNST afferents decreases avoidance of open spaces and respiratory rate, we next investigated which adBNST outputs might mediate these distinct effects. The adBNST projection to the lateral hypothalamus (LH) was a candidate for mediating decreases in behavioural expression of anxiety, as the lateral hypothalamus receives projections from the adBNST but not the ovBNST[18,23,24] (Supplementary Fig. 12a), and is required for normal behaviour in the EPM test25. In agreement with this hypothesis, we found that adBNST neurons projecting to the lateral hypothalamus receive BLA input (Supplementary Fig. 12b–d), and that stimulating the adBNST-LH projection decreased avoidance of open spaces in both the EPM test ($P < 0.01$; Fig. 2f) and the OFT ($P < 0.05$; Supplementary Fig. 9c). However, no effects were seen on respiratory rate (Fig. 2g) or the RTPP test (Fig. 2h), suggesting that the adBNST-LH pathway selectively modulates behavioural, but not physiological or appetitive, features of anxiolysis.

We proposed that the adBNST output to the parabrachial nucleus (PB) could mediate the decrease in respiratory rate seen in ChR2:BLA-adBNST mice (Fig. 2c), as the parabrachial nucleus modulates respiration[2,17,26]. Indeed, in ChR2:BNST-PB mice (Fig. 2i), blue light decreased respiratory rate ($P < 0.05$; Fig. 2k). Furthermore, stimulating the BNST-PB projection attenuated respiratory rate increases in an anxiogenic environment

(Supplementary Fig. 13), but did not change behaviour in the EPM or the RTPP tests (Fig. 2j, l). Although both the adBNST and the ovBNST project to the parabrachial nucleus[18,23,24], the decreased respiratory rate in ChR2:BNST-PB mice was probably driven by adBNST-PB fibres, as ovBNST activity increased the respiratory rate (Fig. 1e and Supplementary Fig. 8). Finally, we tested the adBNST output to the ventral tegmental area (VTA)[18,23,24,27,28] Remarkably, ChR2:adBNST-VTA mice (Fig. 2m) exhibited place preference in the stimulated chamber ($P < 0.001$; Fig. 2p), without affecting anxiety-related risk-avoidance (Fig. 2n) or respiratory rate (Fig. 2o). These data showing complementary roles of different adBNST projections support a model in which populations of adBNST neurons project to distinct downstream structures (lateral hypothalamus, parabrachial nucleus and VTA; Supplementary Fig. 14), modulating different features related to anxiolysis.

We next investigated the intrinsic microcircuitry of the adBNST. To examine connectivity between the BLA and the adBNST, mice expressing ChR2 in the BLA were implanted with a microdrive containing stereotrodes surrounding a fibre-optic in the adBNST (Fig. 3a and Supplementary Fig. 15), allowing simultaneous excitation and recording in awake animals. As expected, excitation of the glutamatergic BLA terminals increased spiking of adBNST single units (Fig. 3b, c), and corresponding whole-cell patch recordings from acute slices revealed that 84% of the adBNST neurons exhibiting both evoked excitatory postsynaptic currents (EPSCs) and inhibitory postsynaptic currents (IPSCs) in voltage clamp (Methods and Supplementary Fig. 16) displayed net excitation in response to BLA input stimulation in current clamp (Fig. 3d–f). Thus, *in vivo* and *in vitro* electrophysiology were concordant in showing that stimulating the BLA-adBNST projection increases adBNST activity, which may be enhanced by local adBNST recurrent excitation (Supplementary Figs 16 and 17). We also characterized local inputs to the adBNST, by recording from adBNST neurons while optically stimulating ovBNST inputs (Fig. 3g). Interestingly, 79% of neurons displayed net inhibition (Fig. 3h, i), consistent with the fact that ovBNST neurons are mostly GABAergic[29]; by contrast, retrograde tracing experiments showed that the adBNST only weakly projects[18,23] to the ovBNST (Supplementary Fig. 18). Together, these data support the conclusion that the ovBNST and adBNST exhibit opposing roles in modulating anxiety.

Next, we asked whether the native firing rates of adBNST neurons in freely moving mice encoded aspects of environmental safety, by recording activity with stereotrode arrays in the adBNST during exploration (Fig. 4a, b). Indeed, greater adBNST multiunit activity was observed in safer locations in two models (closed arms of the EPM test and dark compartment of the light–dark test box; Supplementary Fig. 19). To quantify the extent to which adBNST single units differentiated between closed and open arms in the EPM test, we defined an EPM score (see Supplementary Methods and Supplementary Fig. 20), in which a positive score indicates that firing rates are similar between arms of the same type (such as a pair of closed arms), but different across open and closed arms[30] (for example, Fig. 4c). This metric allowed calculation of specific EPM performance-related activity for each single unit both in light-on and light-off epochs. Without illumination, a subset of adBNST single units fired preferentially in the closed arms of the EPM test, whereas other units did not exhibit preference (Fig. 4c). In fact, every adBNST single unit with a positive EPM score (66% of units) had higher firing rates in the closed arms than in the open arms,

whereas simulations predict that if there were no dependence on environmental condition, only 33% of cells would have a positive EPM score, and those would be evenly divided between closed- and open-arm-preferring units (Supplementary Methods).

We then implanted stereotrodes and a fibre-optic in the adBNST of eNpHR3.0:BLA-adBNST mice (Fig. 4a), allowing simultaneous recording and yellow light delivery to the adBNST. Illumination in these mice reduced multiunit activity in the adBNST (Fig. 4d and Supplementary Fig. 21). Finally, we recorded from adBNST single units in eNpHR3.0:BLA-adBNST mice during the EPM test for 20 min, with alternating 1-min light-off and light-on epochs (Fig. 4e), to allow calculation of EPM scores for each single unit in the presence or absence of inhibition of BLA afferents. Suggesting that representation of anxiety-related features in the adBNST may depend on BLA input, we observed that optogenetic inhibition of the BLA-adBNST projection decreased single-unit EPM scores ($P < 0.01$; Fig. 4f, g), and the decrease in EPM scores was higher in cells that had decreases in the firing rate during the illuminated epochs (Supplementary Fig. 22). These data indicate that native anxiety-related encoding of the EPM environment in the adBNST depends in part on BLA inputs; note that this same manipulation (inhibiting the BLA-adBNST projection) increased anxiety-like behaviour in the EPM test (Fig. 1g), in a manner consistent with causing increased overall anxiety that could deter transitions to the open arm.

Here, we have mapped the role of BNST circuit elements in the assembly and modulation of the anxious behavioural state. We have demonstrated that the ovBNST and adBNST increase and decrease anxiety-related behaviour, respectively; the ovBNST could promote anxiety by suppressing the adBNST (see Supplementary Fig. 23 for summary diagram) or via direct projections to structures such as the central amygdala. We next found that distinct adBNST projections modulate different features of the behavioural state associated with anxiolysis—decreased risk-avoidance behaviour, decreased respiratory rate and positive conditioning valence—which are mediated by projections from the adBNST to the lateral hypothalamus, parabrachial nucleus and VTA, respectively. This arrangement may facilitate modular adaptation of the state itself over development and experience; in principle, by tuning the strength of diverging projections, distinct features may be independently adjusted while maintaining upstream coordination of the behavioural state. Further work will be needed to determine circuit mechanisms by which functional differentiation of these pathways originates, as well as how coordination ultimately occurs. Coordinated recruitment of the different populations of adBNST projection neurons could involve recurrent excitation (Supplementary Figs 16 and 17); indeed, *in vivo* multiunit recordings support the existence of recurrent excitation in the adBNST, as persistent activity was seen in 28% of recordings after termination of BLA fibre stimulation (Supplementary Fig. 17a–c), and Ca^{2+} imaging in acute BNST slice revealed persistent activity in the adBNST after a single brief stimulus (Supplementary Fig. 17d–i).

Many complexities are involved in anxiety, including brain regions, hormonal changes, and physiological manifestations beyond those investigated here. For example, none of our manipulations altered heart rate (Supplementary Fig. 24), consistent with a previous report suggesting the BNST does not modulate this feature of anxiety[17] and pointing to the need for further exploration of sympathetic pathways. Moreover, the anxious state may be parsed

still further to delineate additional features, such as changes in exploratory drive or in novelty seeking, which could involve networks not explored here. It is likely that complex circuit structure and dynamics are required to assemble behavioural states in animals with highly diverse repertoires of internal states and adaptations to the environment.

METHODS SUMMARY

Virus-mediated gene expression.

AAV5 viruses were packaged by the University of North Carolina Vector Core. Maps for the adeno-associated virus constructs are available at http://www.optogenetics.org. Viral stock (0.5 μl) was injected stereotactically into the BLA, BNST, lateral hypothalamus, parabrachial nucleus or VTA.

Anxiety assays and respiratory rate measurement.

Mice injected with viruses and implanted with guide cannulae or fibre-optics were subsequently tested in the EPM test, the OFT and the RTPP test. An EPM test session was 15-min long, consisting of 5-min light off-on-off epochs; the OFT was 20-min long, consisting of 5-min light off-on-off-on epochs. In the RTPP test, the subject could freely explore two chambers, and entry-to or exit-from one of the chambers turned optogenetic stimulation on or off, respectively. Behavioural data were automatically collected and analysed by BiObserve software. Respiratory rate was measured with a pulse oximeter from awake, behaving mice for 3 min. Yellow light was delivered as constant illumination, whereas blue light was delivered as a train of 10-Hz, 5-ms pulses.

In vivo physiology.

Custom-made microdrives containing eight stereotrodes surrounding a fibre-optic were implanted in the BNST, allowing for light delivery and recording of BNST neurons in awake, behaving animals. See Supplementary Methods for further details of analysis and computation of EPM scores.

Ex vivo electrophysiology.

Acute slices were prepared for slice patch-clamp recordings. Whole-cell recordings were conducted from BNST neurons and blue light pulses at 10 Hz were delivered onto coronal sections via the microscope objective.

Statistics.

All graphs and numerical values in the figures are presented as mean ± s.e.m. See Supplementary Information.

Supplementary Material

Refer to Web version on PubMed Central for supplementary material.

Acknowledgements

We thank M. Davis, D. Walker, D. Paré, D. Rainnie, H. Shin, K. Thompson, P. Anikeeva, T. Davidson, I. Goshen, A. Andalman, L. Gunaydin, A. Bryant, C. Lee, J. Mirzabekov and the entire Deisseroth laboratory for discussions. Supported by a Samsung Scholarship (to S.-Y.K.), the US National Institute of Mental Health (NIMH; to R.C.M.), and a Berry Fellowship (to A.A.). K.D. and M.R.W. are NARSAD grant awardees, and K.D. was supported by the Wiegers Family Fund, the NIMH, the US National Institute on Drug Abuse (NIDA), the DARPA REPAIR Program, the Keck Foundation, the McKnight Foundation, the Gatsby Charitable Foundation, the Snyder Foundation, the Woo Foundation, the Tarlton Foundation, and the Albert Yu and Mary Bechman Foundation. All tools and methods are distributed and supported freely (http://www.optogenetics.org).

References

1. LeDoux JE Emotion circuits in the brain. Annu. Rev. Neurosci. 23, 155–184 (2000). [PubMed: 10845062]
2. Davis M The role of the amygdala in fear and anxiety. Annu. Rev. Neurosci. 15, 353–375 (1992). [PubMed: 1575447]
3. LeDoux JE, Iwata J, Cicchetti P & Reis DJ Different projections of the central amygdaloid nucleus mediate autonomic and behavioral correlates of conditioned fear. J. Neurosci. 8, 2517–2529 (1988). [PubMed: 2854842]
4. Viviani D et al. Oxytocin selectively gates fear responses through distinct outputs from the central amygdala. Science 333, 104–107 (2011). [PubMed: 21719680]
5. Kessler RC et al. Lifetime prevalence and age-of-onset distributions of DSM-IV disorders in the National Comorbidity Survey Replication. Arch. Gen. Psychiatry 62, 593–602 (2005). [PubMed: 15939837]
6. Singewald N, Salchner P & Sharp T Induction of c-Fos expression in specific areas of the fear circuitry in rat forebrain by anxiogenic drugs. Biol. Psychiatry 53, 275–283 (2003). [PubMed: 12586446]
7. Dong HW, Petrovich GD & Swanson LW Topography of projections from amygdala to bed nuclei of the stria terminalis. Brain Res. Brain Res. Rev. 38, 192–246 (2001). [PubMed: 11750933]
8. Dabrowska J et al. Neuroanatomical evidence for reciprocal regulation of the corticotrophin-releasing factor and oxytocin systems in the hypothalamus and the bed nucleus of the stria terminalis of the rat: Implications for balancing stress and affect. Psychoneuroendocrinology 36, 1312–1326(2011). [PubMed: 21481539]
9. Walker DL, Miles LA & Davis M Selective participation of the bed nucleus of the stria terminalis and CRF in sustained anxiety-like versus phasic fear-like responses. Prog. Neuropsychopharmacol. Biol. Psychiatry 33, 1291–1308 (2009). [PubMed: 19595731]
10. Duvarci S, Bauer EP & Paré D The bed nucleus of the stria terminalis mediates inter-individual variations in anxiety and fear. J. Neurosci. 29,10357–10361 (2009). [PubMed: 19692610]
11. Yassa MA, Hazlett RL, Stark CEL & Hoehn-Saric R Functional MRI of the amygdala and bed nucleus of the stria terminalis during conditions of uncertainty in generalized anxiety disorder. J. Psychiatr. Res. 46, 1045–1052 (2012). [PubMed: 22575329]
12. Straube T, Mentzel H-J & Miltner WHR Waiting for spiders: brain activation during anticipatory anxiety in spider phobics. Neuroimage 37, 1427–1436(2007). [PubMed: 17681799]
13. Carola V, D'Olimpio F, Brunamonti E, Mangia F & Renzi P Evaluation of the elevated plus-maze and open-field tests for the assessment of anxiety-related behaviour in inbred mice. Behav. Brain Res. 134, 49–57 (2002). [PubMed: 12191791]
14. Gradinaru V et al. Molecular and cellular approaches for diversifying and extending optogenetics. Cell 141, 154–165 (2010). [PubMed: 20303157]
15. Martin B The assessment of anxiety by physiological behavioral measures. Psychol. Bull. 58, 234–255 (1961). [PubMed: 13767312]
16. Suess WM, Alexander AB, Smith DD, Sweeney HW& Marion RJ. The effects of psychological stress on respiration: a preliminary study of anxiety and hyperventilation. Psychophysiology 17, 535–540 (1980). [PubMed: 7443919]

17. Terreberry RR, Oguri M& Harper RM. State-dependent respiratory and cardiac relationships with neuronal discharge in the bed nucleus of the stria terminalis. Sleep 18, 139–144 (1995). [PubMed: 7610308]
18. Dong H-W & Swanson LW Organization of axonal projections from the anterolateral area of the bed nuclei of the stria terminalis. J. Comp. Neurol. 468, 277–298 (2004). [PubMed: 14648685]
19. Dunn JD & Williams TJ Cardiovascular responses to electrical stimulation of the bed nucleus of the stria terminalis. J. Comp. Neurol. 352, 227–234 (1995). [PubMed: 7721991]
20. Dunn JD Plasma corticosterone responses to electrical stimulation of the bed nucleus of the stria terminalis. Brain Res. 407, 327–331 (1987). [PubMed: 3567648]
21. Woods JH, Katz JL & Winger G Benzodiazepines: use, abuse, and consequences. Pharmacol. Rev. 44, 151–347 (1992). [PubMed: 1356276]
22. Koob GF A role for brain stress systems in addiction. Neuron 59, 11–34 (2008). [PubMed: 18614026]
23. Dong H-W & Swanson LW Projections from bed nuclei of the stria terminalis, anteromedial area: cerebral hemisphere integration of neuroendocrine, autonomic, and behavioral aspects of energy balance. J. Comp. Neurol. 494, 142–178 (2006). [PubMed: 16304685]
24. Dong HW, Petrovich GD, Watts AG & Swanson LW Basic organization of projections from the oval and fusiform nuclei of the bed nuclei of the stria terminalis in adult rat brain. J. Comp. Neurol. 436, 430–455 (2001). [PubMed: 11447588]
25. Hakvoort Schwerdtfeger RM & Menard JL The lateral hypothalamus and anterior hypothalamic nucleus differentially contribute to rats' defensive responses in the elevated plus-maze and shock-probe burying tests. Physiol. Behav. 93, 697–705 (2008). [PubMed: 18164736]
26. Chamberlin NL & Saper CB Topographic organization of respiratory responses to glutamate microstimulation of the parabrachial nucleus in the rat. J. Neurosci. 14, 6500–6510(1994). [PubMed: 7965054]
27. Sartor GC & Aston-Jones G Regulation of the ventral tegmental area by the bed nucleus of the stria terminalis is required for expression of cocaine preference. Eur. J. Neurosci. 36, 3549–3558 (2012). [PubMed: 23039920]
28. Georges F & Aston-Jones G Activation of ventral tegmental area cells by the bed nucleus of the stria terminalis: a novel excitatory amino acid input to midbrain dopamine neurons. J. Neurosci. 22, 5173–5187 (2002). [PubMed: 12077212]
29. Poulin J-F, Arbour D, Laforest S & Drolet G Neuroanatomical characterization of endogenous opioids in the bed nucleus of the stria terminalis. Prog. Neuropsychopharmacol. Biol. Psychiatry 33, 1356–1365 (2009). [PubMed: 19583989]
30. Adhikari A, Topiwala MA & Gordon JA Single units in the medial prefrontal cortex with anxiety-related firing patterns are preferentially influenced by ventral hippocampal activity. Neuron 71, 898–910 (2011). [PubMed: 21903082]

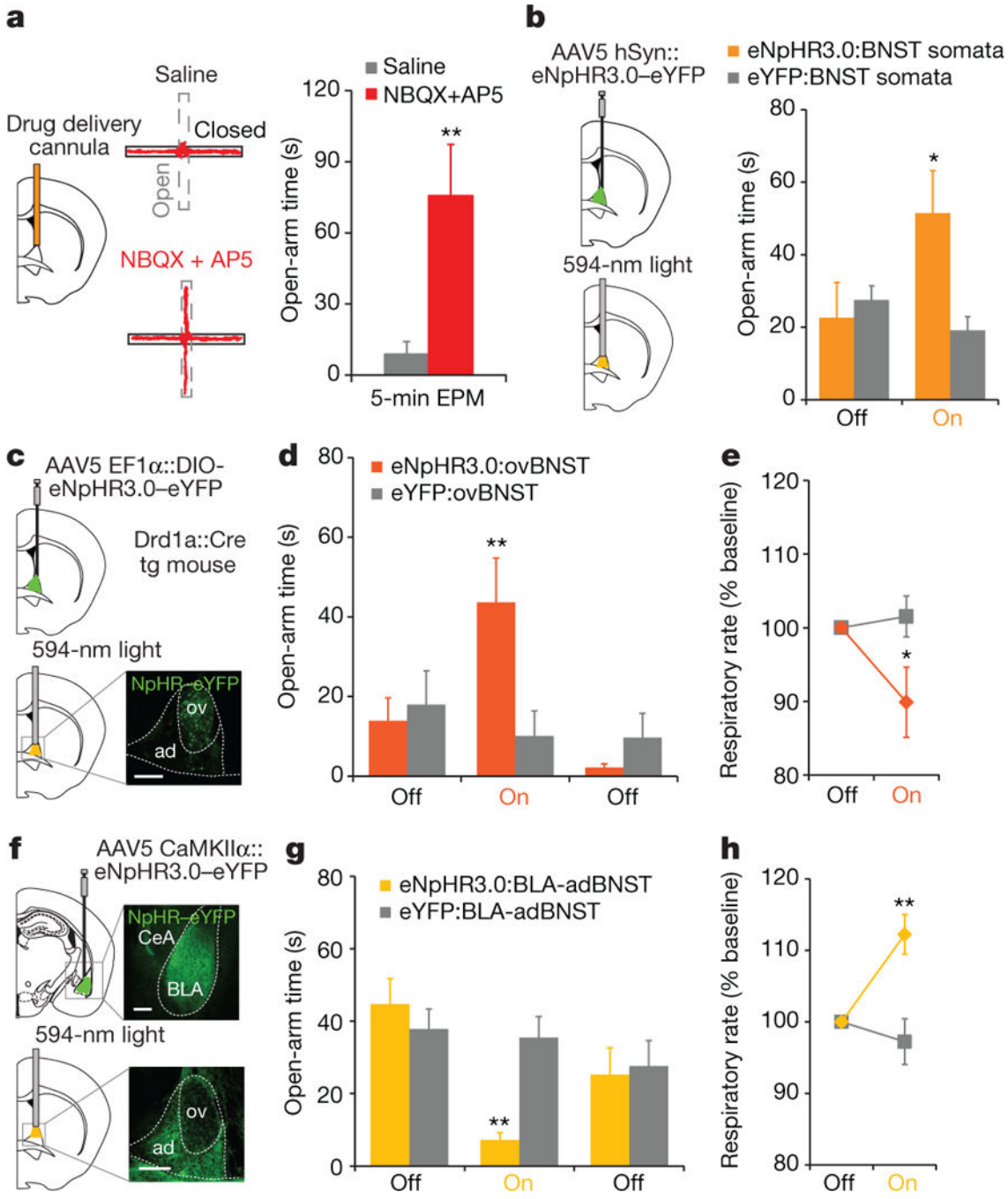

Figure 1 |. Functional heterogeneity within the dorsal BNST.

a, Cannula for drug infusion; NBQX (2,3-dioxo-6-nitro-1,2,3,4-tetrahydrobenzo[f]quinoxaline-7-sulphonamide) plus AP5 (D(−)-2-amino-5-phosphonovaleric acid) increased open-arm time in the EPMtest ($n = 5$ for each). **b**, eNpHR3.0:BNST somata mice were bilaterally implanted with fibre-optics above the BNST. Light increased open-arm time in the EPM test ($n = 8$ eNpHR3.0, $n = 8$ eYFP). eNpHR3.0–eYFP was under the control of the human synapsin 1 promoter (adeno-associated virus type 5 (AAV5) human synapsin promoter fragment (hSyn)::eNpHR3.0–eYFP). **c**,

eNpHR3.0:ovBNST mice received bilateral light. ovBNST-restricted expression was obtained with Cre-dependent eNpHR3.0 adeno-associated virus in Drd1a::Cre transgenic (tg) mice. eNpHR3.0–eYFP was under the control of the EF1α promoter. **d, e**, Light delivery to ovBNST of eNpHR3.0:ovBNST mice increased open-arm time in the EPM test (n = 7 eNpHR3.0, n = 8 eYFP) (**d**) and decreased respiratory rate (n = 7 eNpHR3.0, n = 8 eYFP) (e). **f**, eNpHR3.0:BLA-adBNSTmice expressing eNpHR3.0 in BLA received bilateral illumination of BLA fibres in adBNST. eNpHR3.0–eYFP was under the control of the CaMKIIa promoter. **g, h**, Light in eNpHR3.0:BLAadBNST mice reduced open-arm time (n = 11 eNpHR3.0, n = 15 eYFP) (**g**) and increased respiratory rate (n = 8 eNpHR3.0, n = 8 eYFP) (**h**). Scale bars, 200 μm. Data are mean ± s.e.m. *P < 0.05; **P < 0.01. Statistics in Supplementary Information; see also Supplementary Fig. 5.

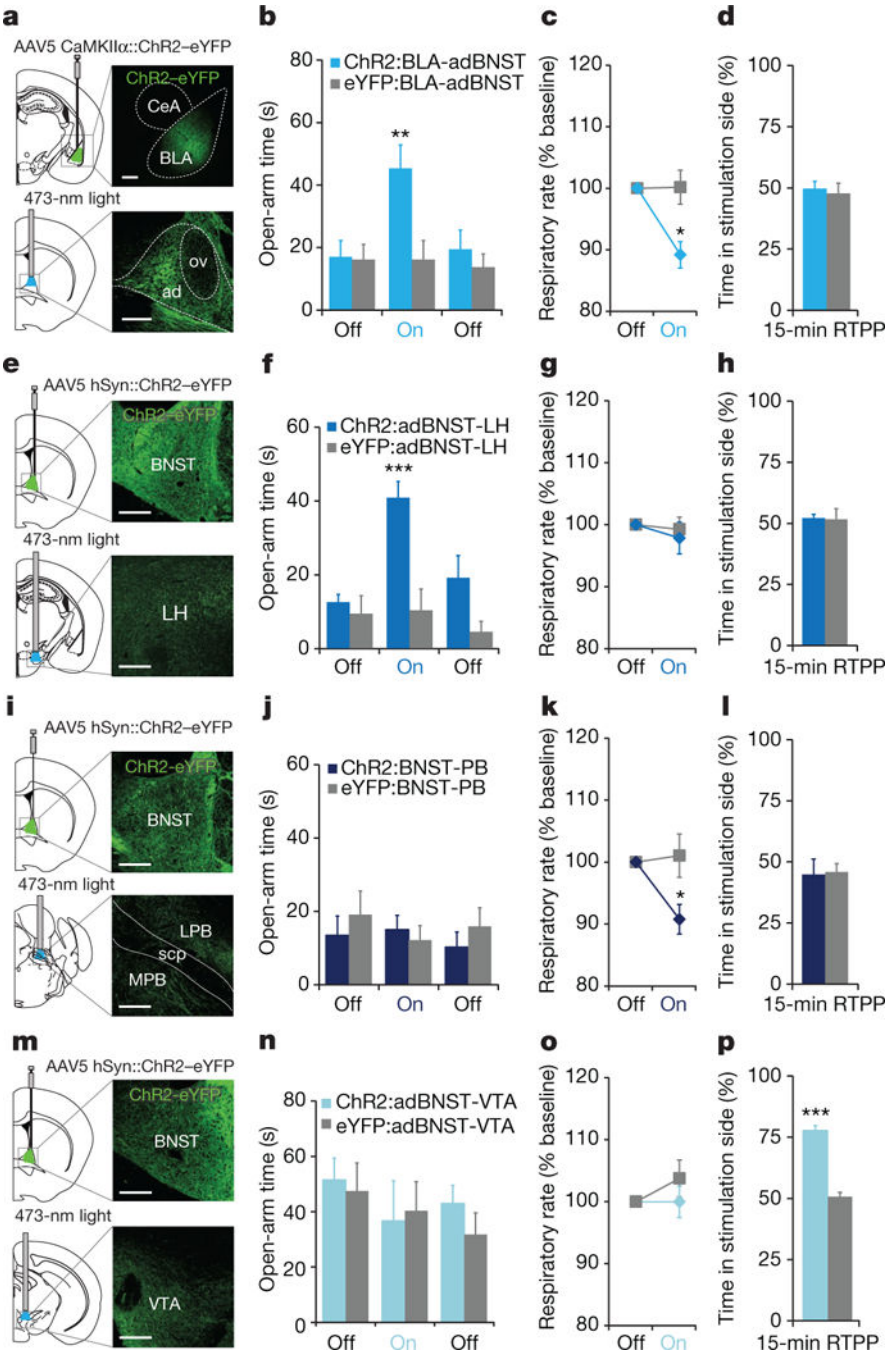

Figure 2 |. Distinct adBNST outputs modulate different features related to anxiolysis.

a, ChR2:BLA-adBNST mice were transduced in BLA, and unilateral fibre-optics implanted above BLA fibres in adBNST. CeA, central amygdala. **b–d**, Light to adBNST increased open-arm time in the EPM test (n = 11 ChR2, n = 12 eYFP) (**b**) and decreased respiratory rate (n = 7 ChR2, n = 8 eYFP) (**c**), but did not elicit place preference (n = 8 ChR2, n = 6 eYFP) (**d**). **e**, ChR2:adBNST-LH mice were transduced in BNST, and unilateral fibre-optics implanted above the lateral hypothalamus. **f–h**, In ChR2:adBNST-LH mice, light increased the open-arm time in the EPM test (n = 11 ChR2, n = 8 eYFP) (**f**), but did not affect

respiratory rate (n = 9 ChR2, n = 10 eYFP) (**g**) or place preference (n = 7 ChR2, n = 7 eYFP) (**h**). **i**, ChR2:BNST-PB mice were transduced in BNST, and unilateral fibre-optics implanted in the parabrachial nucleus. LPB, lateral parabrachial nucleus; MPB, medial parabrachial nucleus; scp, superior cerebellar peduncle. **j–l**, Light in ChR2:BNST-PB mice did not influence performance in the EPM test (n = 7 ChR2, n = 7 eYFP) (**j**), but decreased respiratory rate (n = 8 ChR2, n = 7 eYFP) (**k**); no effect was seen on place preference (n = 7 ChR2, n = 5 eYFP) (**l**). **m**, ChR2:adBNST-VTA mice were transduced in the BNST, and unilateral fibre-optics implanted directly above the VTA. **n–p**, Light did not affect the EPM test (n = 7 ChR2, n = 7 eYFP) (**n**) or respiratory rate (n = 8 ChR2, n = 7 eYFP) (**o**), but induced robust place preference (n = 8 ChR2, n = 7 eYFP) (**p**). Scale bars, 200 μm. Data are mean ± s.e.m. *P < 0.05; **P < 0.01; ***P < 0.001. Statistics in Supplementary Information; see also Supplementary Fig. 9.

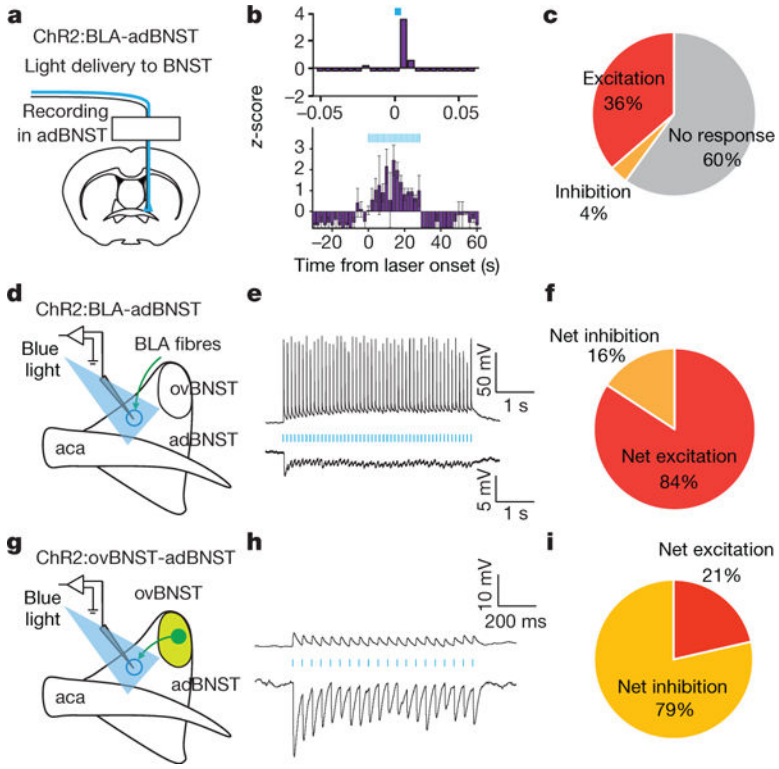

Figure 3 |. *In vivo* and *in vitro* electrophysiological assessment of adBNST afferents.

a–f, Assessment of BLA afferents to adBNST. **a**, ChR2:BLA-adBNST mice were implanted with a microdrive containing eight stereotrodes and a fibre-optic in adBNST to allow simultaneous optogenetic stimulation and recording of adBNST neurons. **b**, Representative peristimulus time histograms of adBNST single units in behaving mice, showing typical responses to 5-ms light pulse (top), and to a 10-Hz light-pulse train for 20 s (bottom). **c**, Excitation was most commonly observed ($n = 55$). **d**, ChR2 was expressed in the BLA; acute slices were prepared from the BNST, and BNST neurons were recorded in current-clamp while optically stimulating BLA afferents. aca, anterior commissure. **e**, Representative traces from adBNST neurons ($V_m \approx -60$ mV), displaying excitatory (top) and inhibitory (bottom) responses. **f**, Among adBNST neurons that showed both EPSCs and IPSCs, most were excited at resting potential ($n = 16$ out of 19 neurons; see Supplementary Fig. 16 for voltage-clamp). **g–i**, Electrophysiologically assessed functional connectivity from ovBNST to adBNST (Supplementary Fig. 18 illustrates minimal connectivity in the reverse direction). **g**, ChR2 was expressed in ovBNST using transgenic Drd1a::Cre mice; adBNST neurons were recorded while stimulating ovBNST fibres. **h**, Representative current-clamp traces from adBNST neurons ($V_m \approx -60$ mV), exhibiting excitatory (top) and inhibitory (bottom) responses. **i**, Among adBNST neurons that showed both EPSCs and IPSCs, most were inhibited at resting potential ($n = 11$ out of 14 neurons). Data are mean ± s.e.m. Statistics in Supplementary Information.

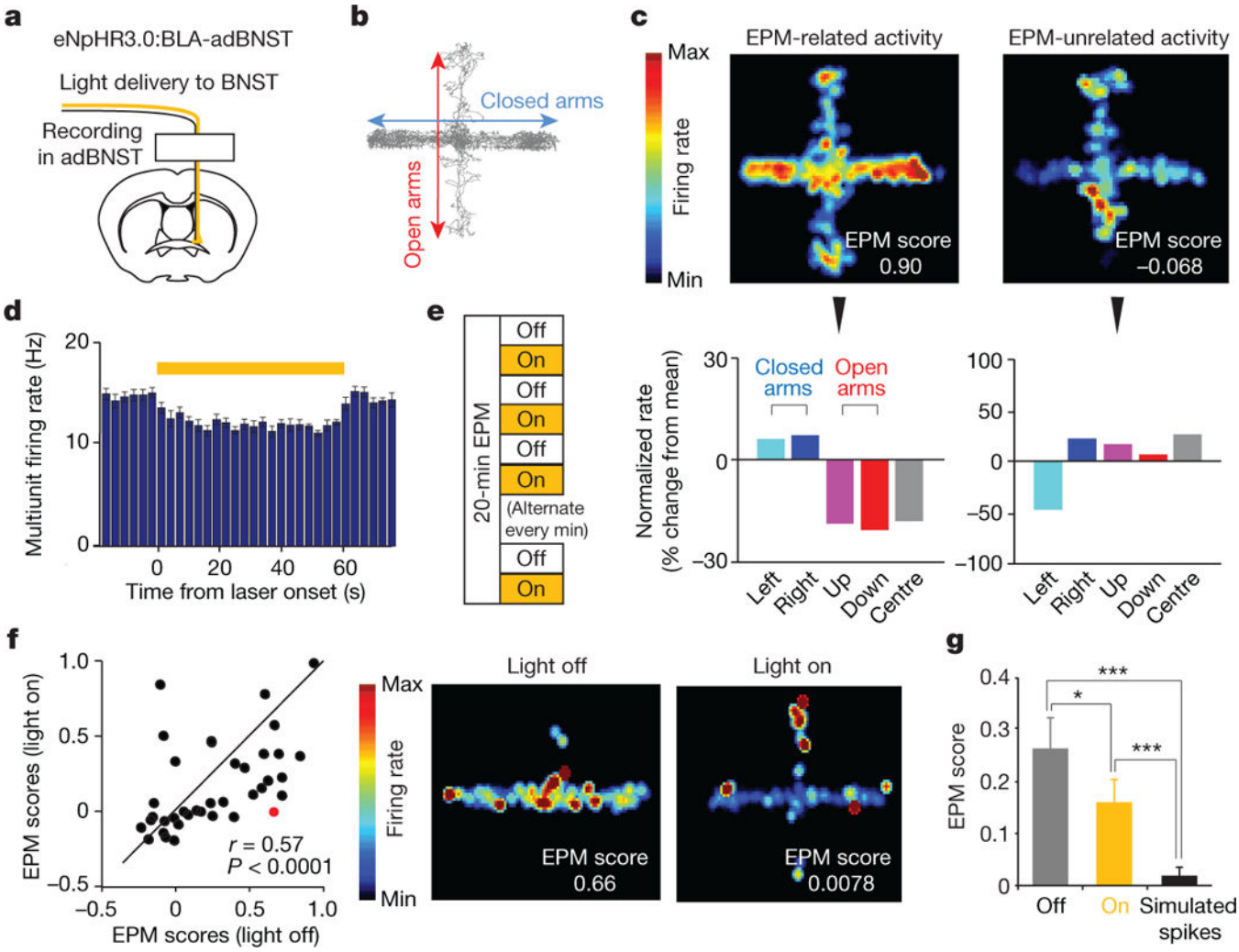

Figure 4 |. BNST neurons rely in part on BLA inputs to distinguish safe and anxiogenic locations.

a, Schematic of *in vivo* recording configuration. **b**, Representative behavioural track tracing from the EPM test. For all EPM figures, horizontal and vertical arms represent closed and open arms, respectively. **c**, Top, spatial firing rate maps of two representative adBNST single units. One unit showed higher activity in closed arms (left), whereas the other did not exhibit preference (right); average normalized firing rates are colour-coded for each pixel of spatial location. Bottom, normalized rates (percentage change from mean firing rate) for each arm for example units. These rates were used to calculate EPM scores (Supplementary Methods and Supplementary Fig. 20); higher EPM scores indicate greater differentiation of closed and open arms. **d**, Light to inhibit the BLA-adBNST projection modestly suppressed multiunit activity in adBNST. **e**, eNpHR3.0:BLA-adBNST mice were run in the EPM test for 20 min with alternating 1-min light-off and light-on epochs. **f**, Left, scatterplot of EPM scores in light-off and light-on conditions. Right, spatial firing maps illustrating change in EPM score of one single unit (red point in scatterplot) in response to yellow light, which decreased EPM score of most (n = 28 out of 38) units. **g**, Summary data across single units (n = 38): mean change in EPM score with inhibition of the adBNST projection. Notably, EPM scores even in light-on epochs were significantly higher than EPM scores generated

from random simulated spikes ($P < 0.01$), indicating that even in light-on, BNST units could differentiate closed and open arms, although less robustly than in light-off. Data are mean ± s.e.m. *$P < 0.05$; ***$P < 0.001$. Statistics in Supplementary Information.